

The results pertaining to the experiments carried out as mentioned in chapter-III using treated *Terminalia catappa* fruit shells (TTCNS) and treated *Azadirachta indica* seed shells (TAINS) to remove Ni(II) from aqueous solutions and industrial effluents are discussed below.

4.1 BET and BJH Analysis

BET and BJH methods are used for the evaluation of the particle and mesopore size distribution. Pore sizes are classified in accordance with the classification adopted by the International Union of Pure and Applied Chemistry (IUPAC)²¹³, that is, micropores (diameter $d < 20 \text{Å}$), mesopores ($20 \text{Å} < d < 500 \text{Å}$) and macropores ($d > 500 \text{Å}$). Micropores can be divided into ultra-micropores ($d < 7 \text{Å}$) and super-micropores ($7 \text{Å} < d < 20 \text{Å}$). Because of the larger sizes of liquid molecules, the adsorbents for liquid phase adsorbates should have predominantly mesopores in the structure²¹⁴. TTCNS and TAINS have wide pore size distribution (Figures 4.1 and 4.2) with enlarged surface area. The BET surface area of TTCNS is $83.14 \text{m}^2/\text{g}$ and the mean pore diameter is found to be 386.91Å . BET analysis of TAINS depicted a surface area of $28.81 \text{m}^2/\text{g}$ and average pore diameter of 147.65Å whereas BJH adsorption/desorption total pore volume is $6.80 \text{cm}^3/\text{g}$. The BJH adsorption/desorption total pore volume of TAINS is found to be $5.90 \text{cm}^3/\text{g}$. Thus, both TTCNS and TAINS is found to possess mesopores predominantly, as their pore diameter lie in the range of $20 \text{Å} < d < 500 \text{Å}$. This is found to be desirable for the liquid phase adsorptive removal of metal ions, indicating the predominance of mesopores in adsorption process.

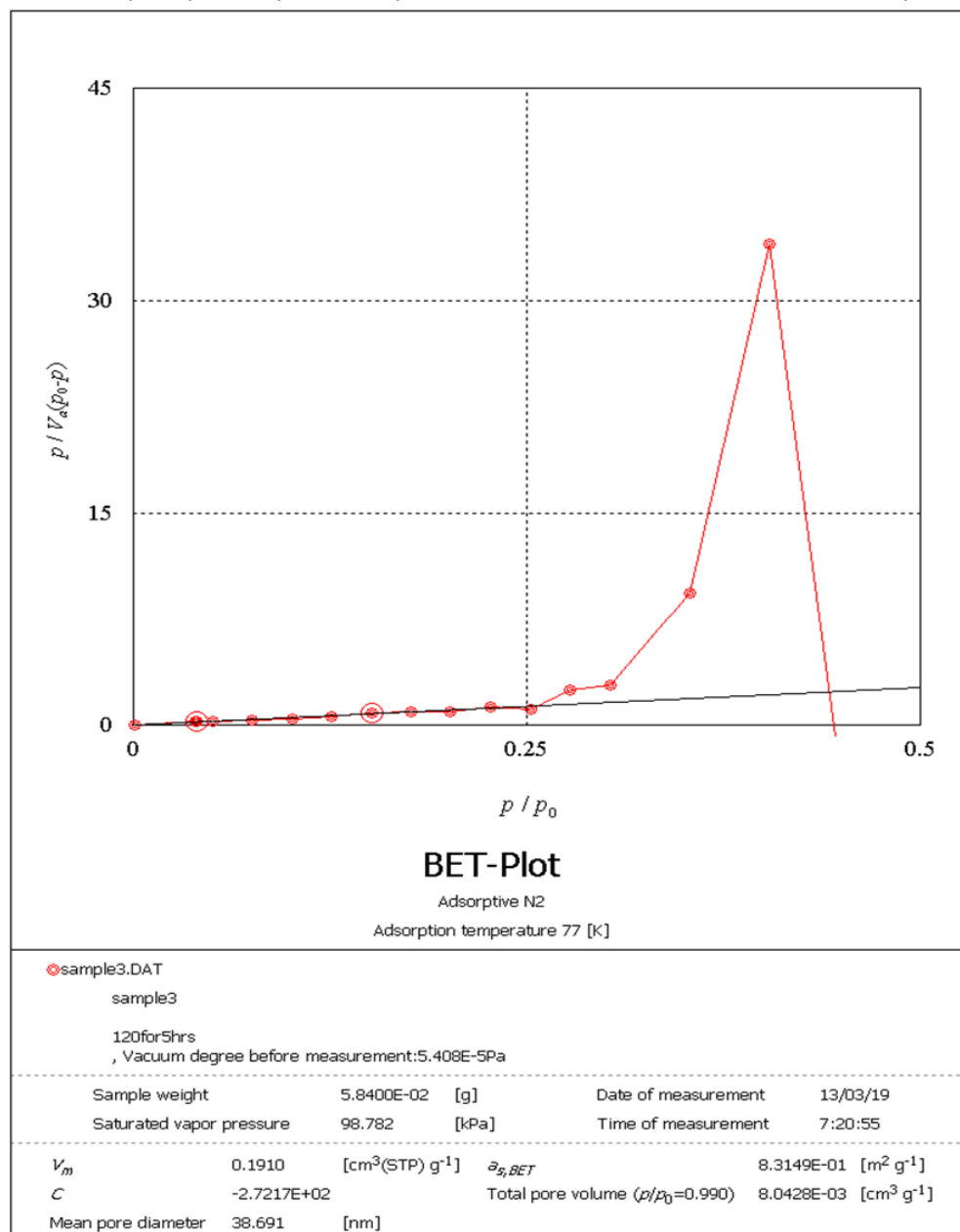


Figure 4.1 BET plot for TTCNS

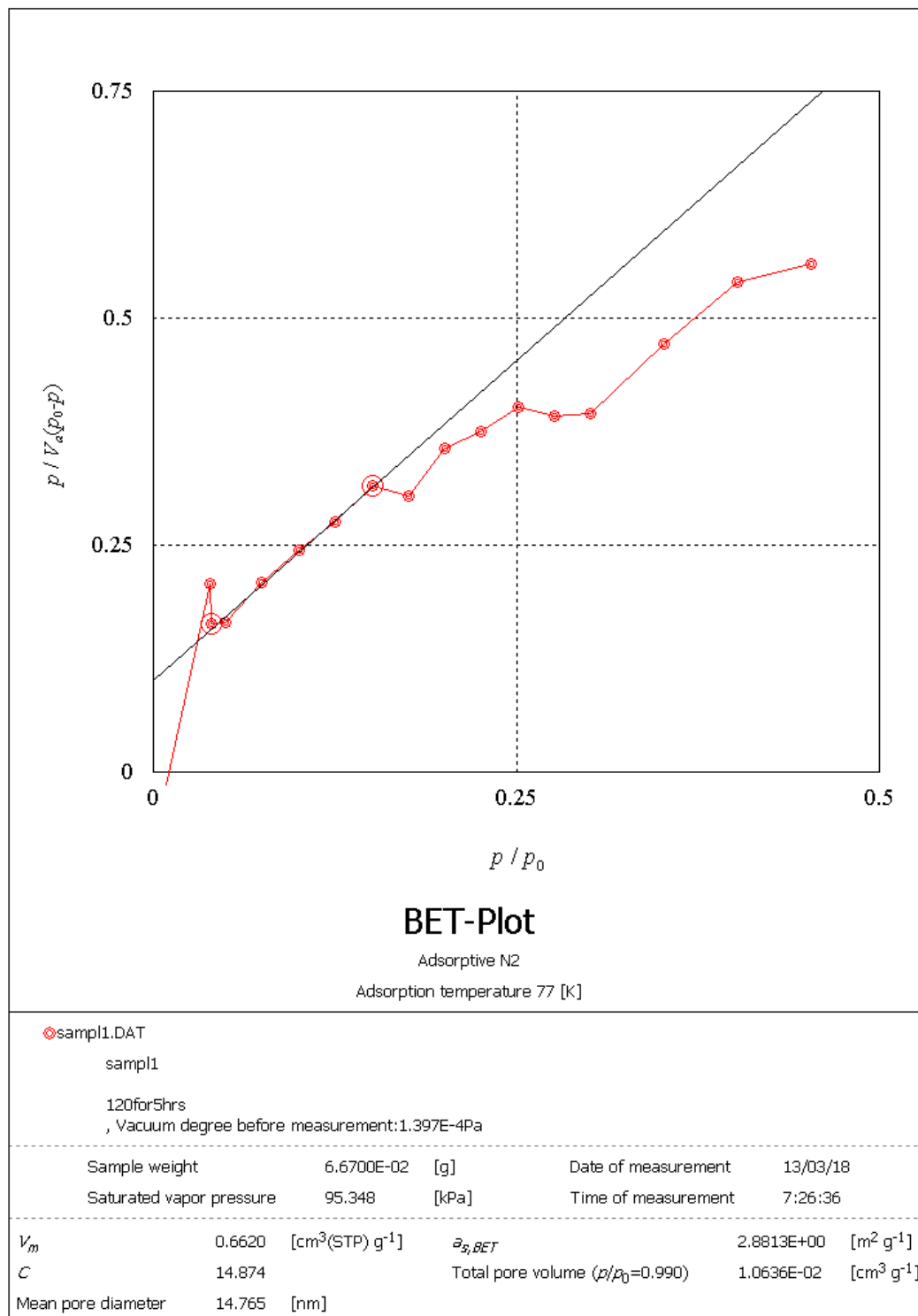


Figure 4.2 BET plot for TAINS

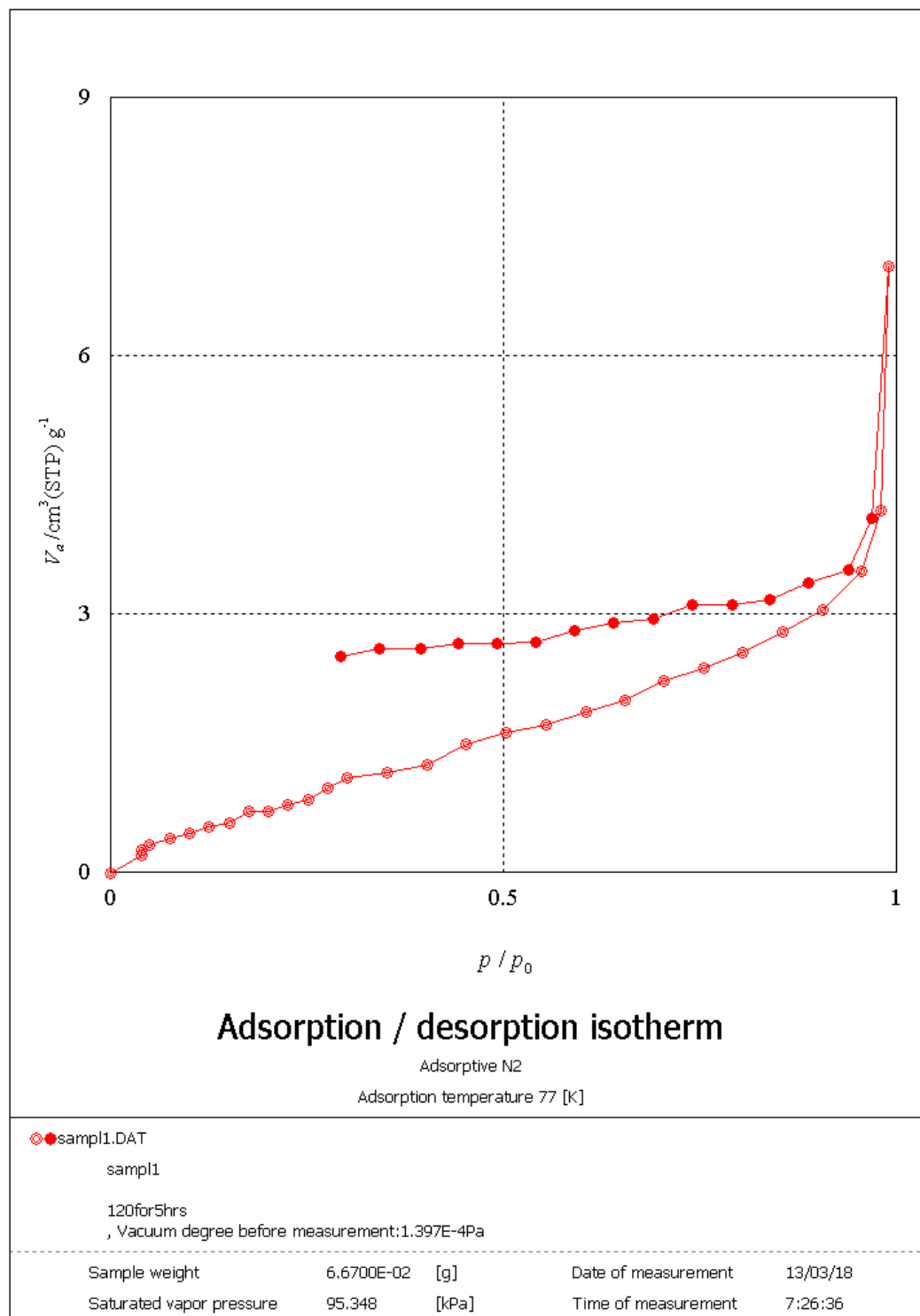


Figure 4.3 BJH plot for TTCNS

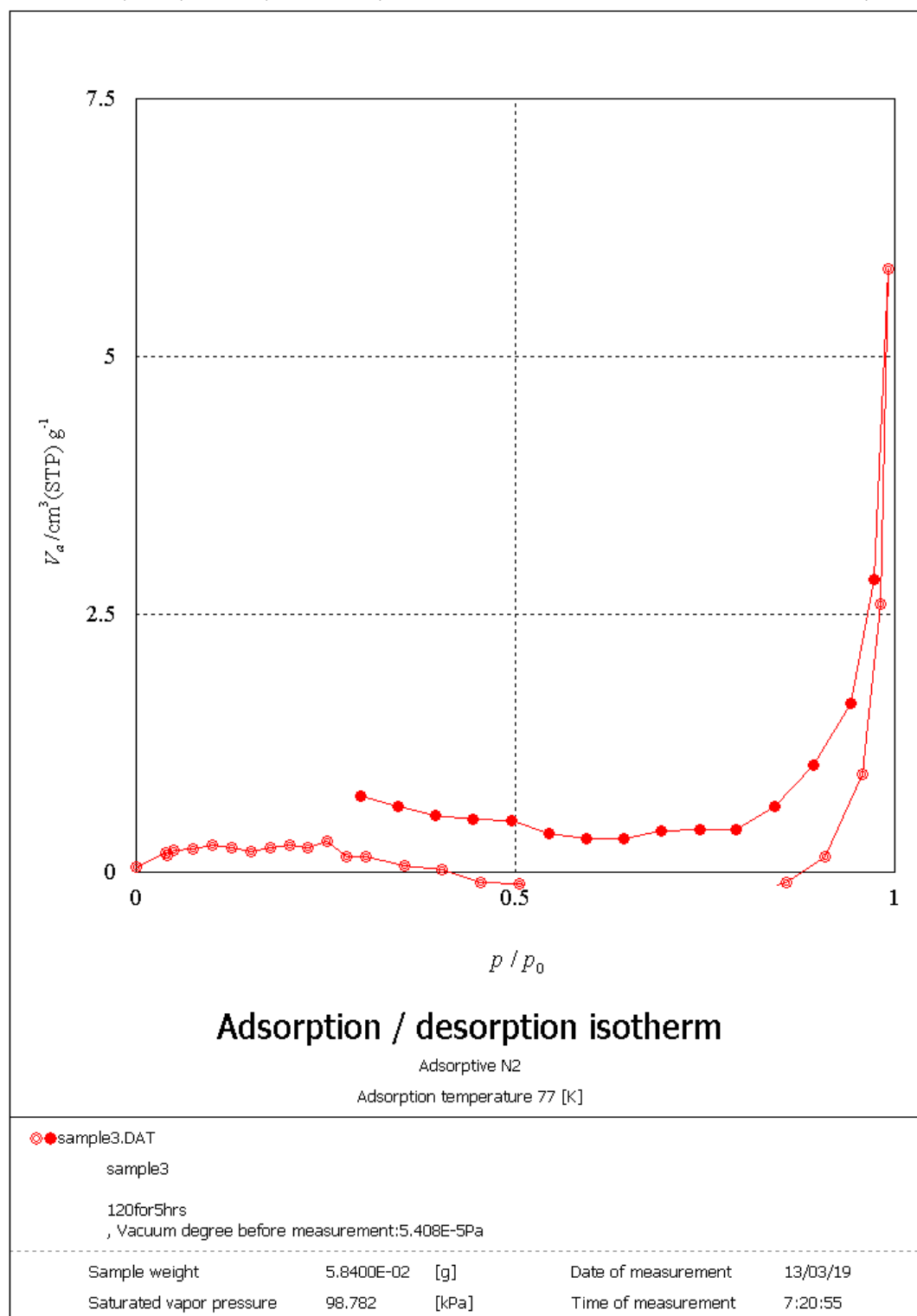


Figure 4.4 BJH plot for TAINS

4.2 SEM and EDAX Analysis

The scanning electron micrographs enable the direct observation of the surface microstructures of different adsorbents. The surface morphology of the adsorbents was visualized using Scanning Electron Microscope (SEM) and the images with suitable magnification are presented. SEM pictures of the unloaded adsorbents are illustrated in figures 4.5, 4.7 and the Ni(II) loaded adsorbents are given in figures 4.6, 4.8 respectively. The surface of the pure adsorbent is smooth and homogeneous. In Ni(II) loaded SEM pictures, the smoothness and rugosity of the surface is disturbed.

The Energy dispersive X-ray Analysis (EDAX) of the samples were recorded for qualitative analysis of the elemental constitution of the adsorbents. The EDAX spectra of both unloaded and loaded adsorbents are depicted in figures 4.9-4.12. The presence of peak for nickel in the corresponding spectra substantiate the adsorption of Ni(II) onto TTCNS and TAINS.

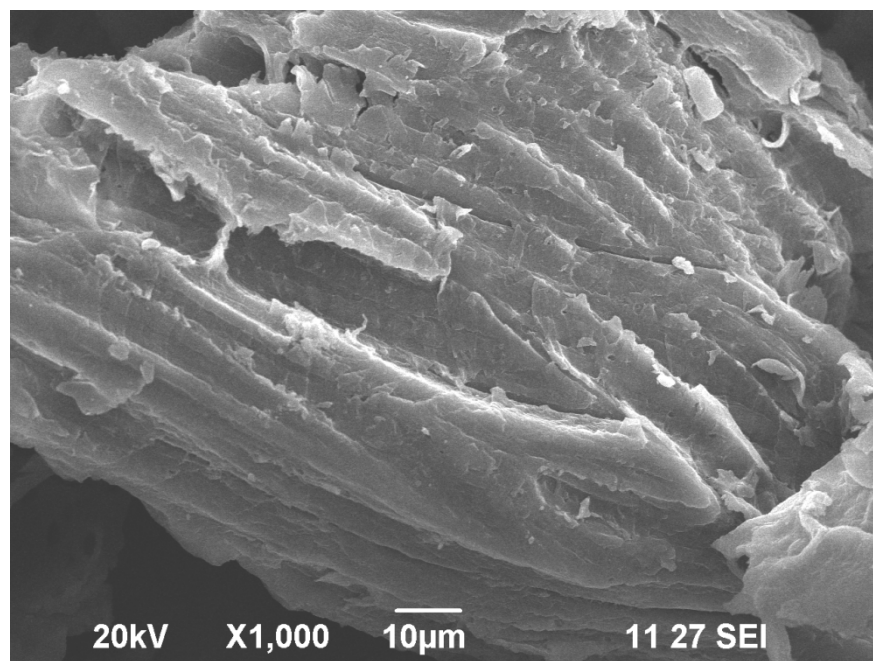


Figure 4.5 SEM of TTCNS

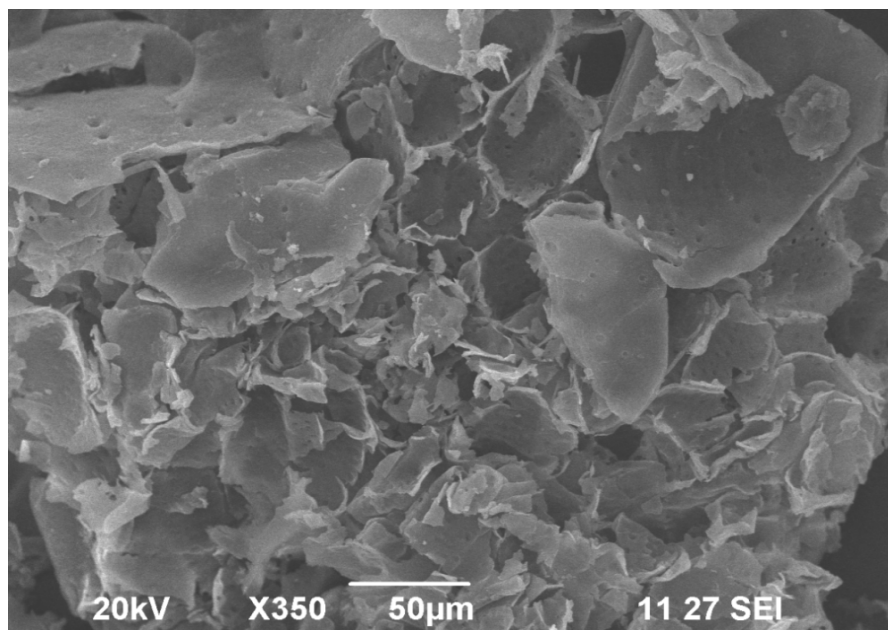


Figure 4.6 SEM of Ni(II) loaded TTCNS

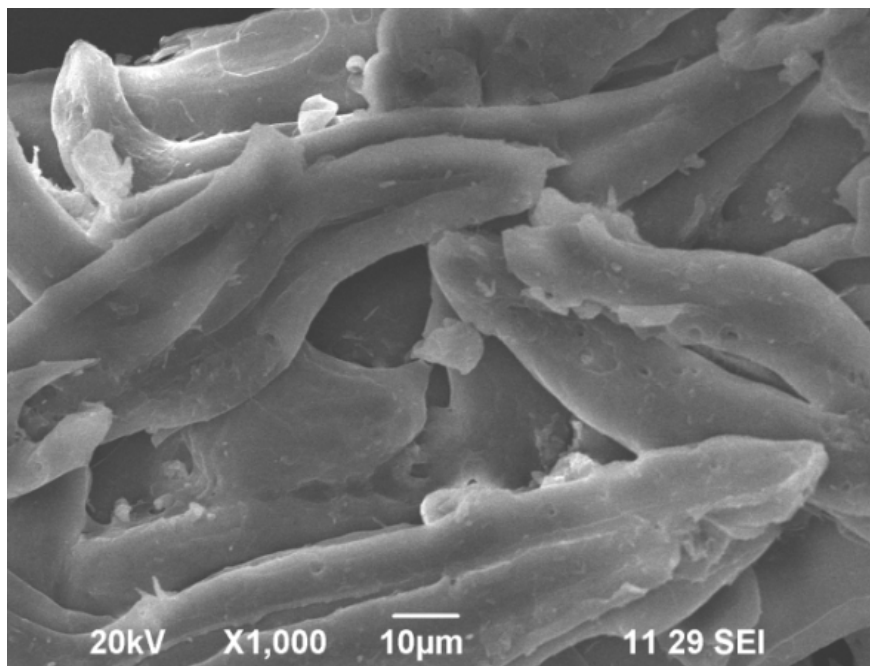


Figure 4.7 SEM of TAINS

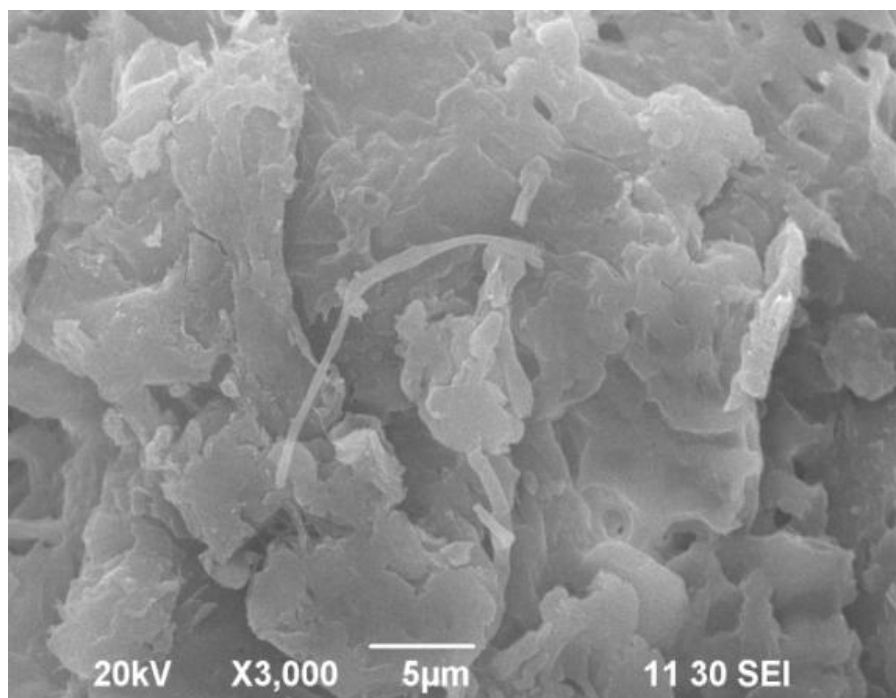


Figure 4.8 SEM of Ni(II) loaded TAINS

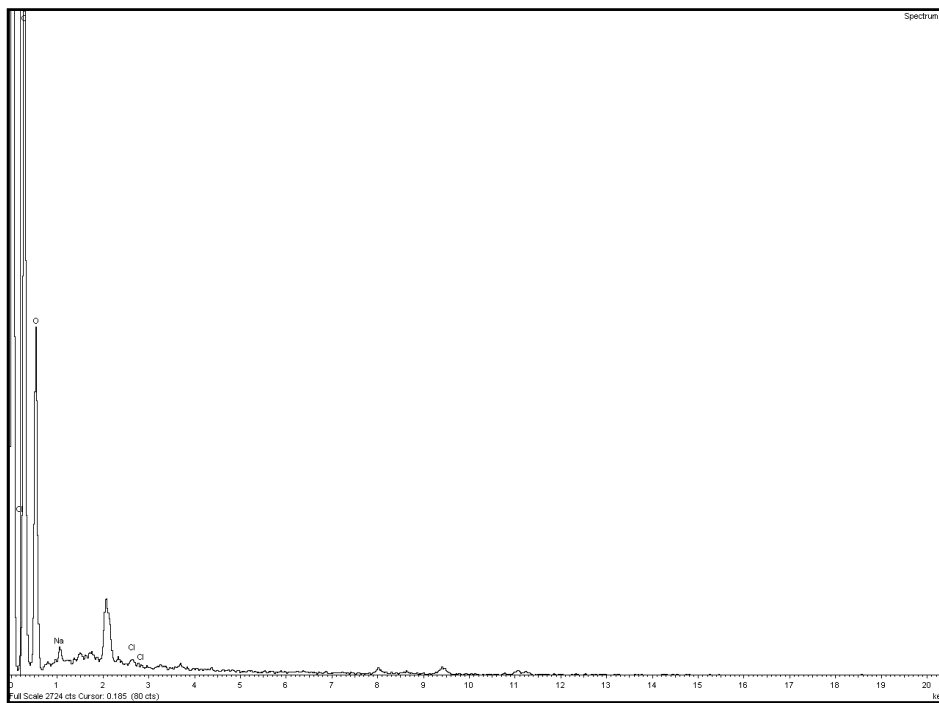


Figure 4.9 EDAX spectrum of TTCNS

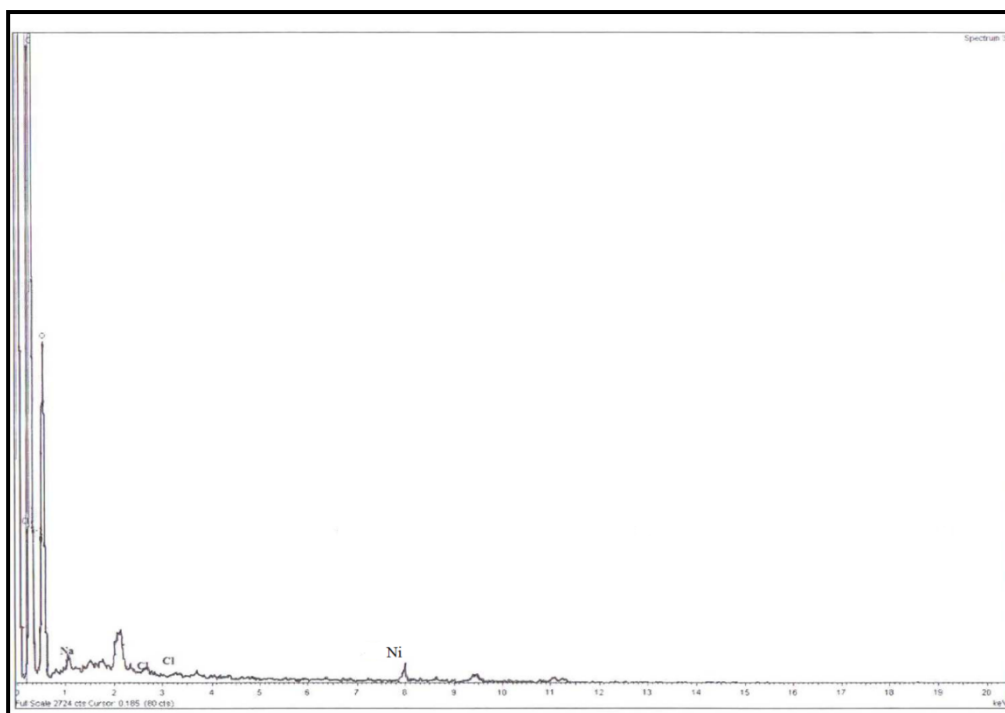


Figure 4.10 EDAX spectrum of Ni(II) loaded TTCNS

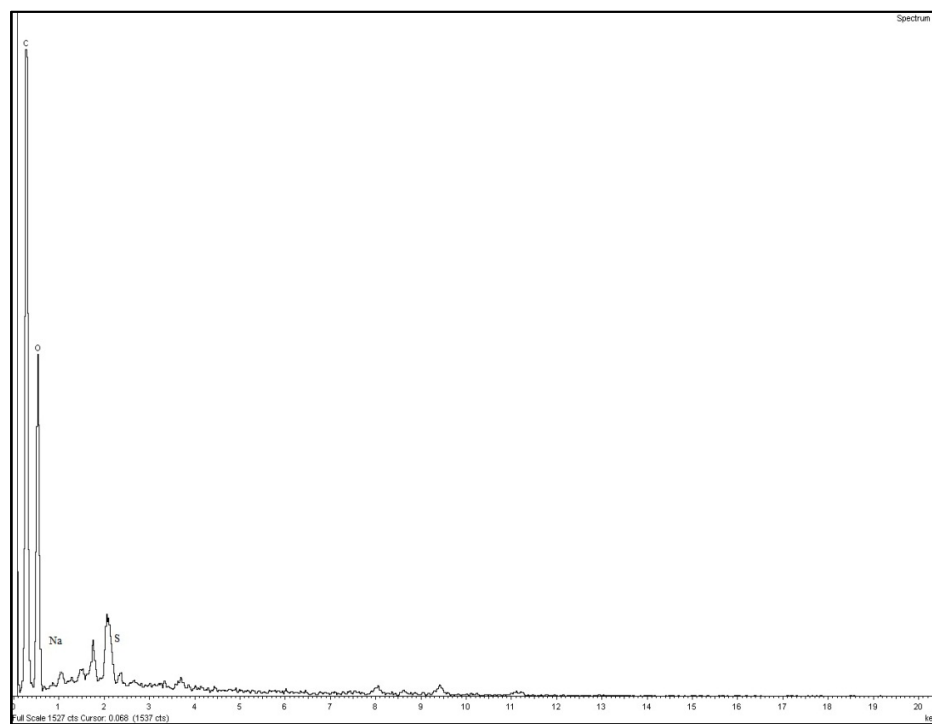


Figure 4.11 EDAX spectrum of TAINS

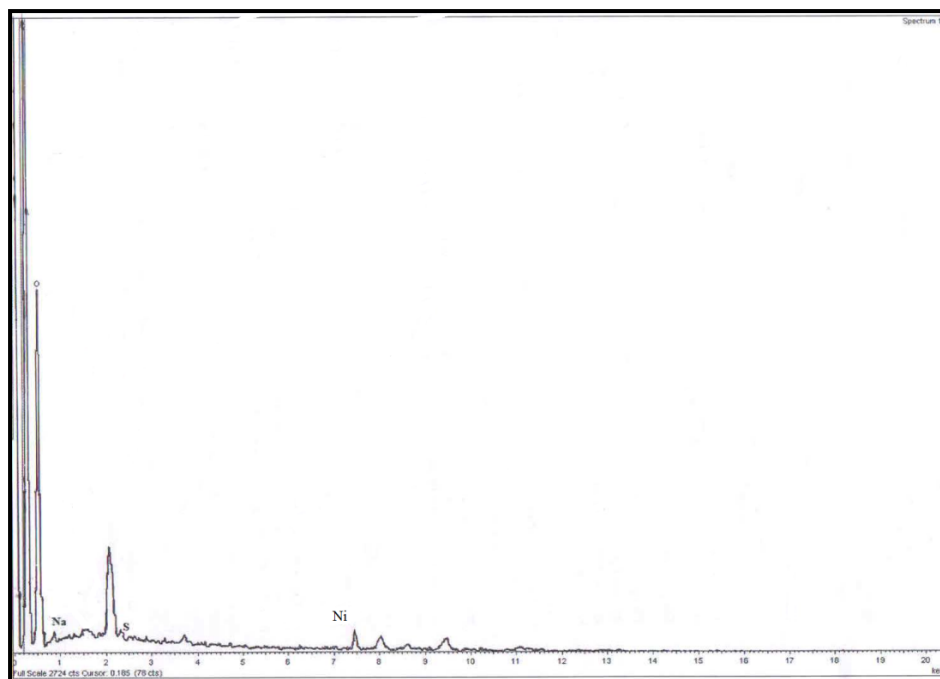


Figure 4.12 EDAX spectrum of Ni(II) loaded TAINS

4.3 FT-IR Spectral Analysis

The FT-IR spectrum shows the functional groups which are present on the surface of the adsorbents. However, the availability of a particular functional group or binding site does not necessarily guarantee its accessibility as an adsorption site for a metal ion, because of the presence of steric, conformational or other types of barriers.

The FT-IR spectra of TTCNS and TAINS before and after Ni(II) adsorption are presented in figures 4.13- 4.16. The spectra display few absorption peaks corresponding to different functional groups. The infra-red spectra of the adsorbent samples were measured as potassium bromide pellets using a Shimadzu 8400S FTIR spectrometer.

The FT-IR spectra of unloaded and Ni(II) loaded TTCNS material are shown in figures 4.13 and 4.14 respectively. The adsorption peak around 3650.96 cm^{-1} (Fig 4.15) indicates the existence of free and intermolecular bonded hydroxyl groups which was not present after nickel exposure (Fig 4.14) indicating participation of these functionalities in metal binding²¹⁵. The band observed at around 1604.34 cm^{-1} (Fig 4.13) due to C=O stretching, (characteristic of esters) in the spectra of the unloaded sample is shifted to 1637.23 cm^{-1} (Fig 4.14) corresponding to the loaded one. This may be due to the cleavage of bonds because of the hydrolysis of ester to acid in metal loaded adsorbent. A decrease in final pH of Ni(II) loaded adsorbent indicates that -COOH group thus obtained could be the metal binding site resulting in the release of H^+ ions in solution.

Examination of the spectra of TAINS before and after Ni(II) adsorption shows the following shift in absorption peaks (Fig 4.15 and 4.16). For unloaded TAINS, the band at region 3411.97 cm^{-1} corresponds to O-H stretching of polymeric compounds, 2920.71 cm^{-1} is symmetric vibration of CH_2 , 1638.04 cm^{-1} is stretching vibration of C=O, 1508.40 cm^{-1} band is stretching vibration of C-N of peptidic bond of proteins, 1325.42 cm^{-1} band is vibration of phosphate groups, 1233.02 cm^{-1} band is due to the vibration of carboxylic acids. The probable functional groups which may play a key role in the adsorption sites of

TAINSShall be C=O at 1638.04 cm^{-1} which is shifted to 1596.22 cm^{-1} and O-H at 3411.97 cm^{-1} which is shifted to 3363.47 cm^{-1} as observed in the spectral peaks of Ni(II) loaded adsorbents. Similar observation has been reported by Sheng et al., supporting this spectral study²¹⁶.

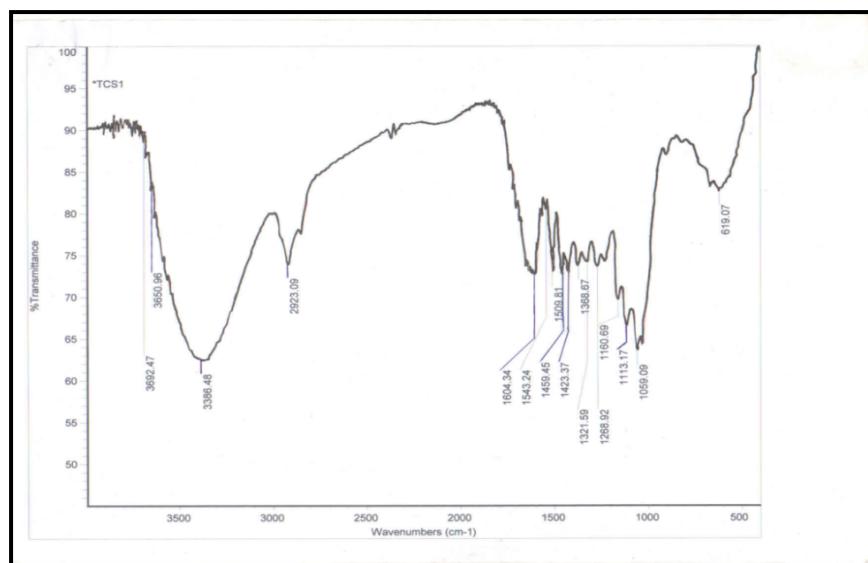


Figure 4.13 FT-IR spectrum of TTCNS

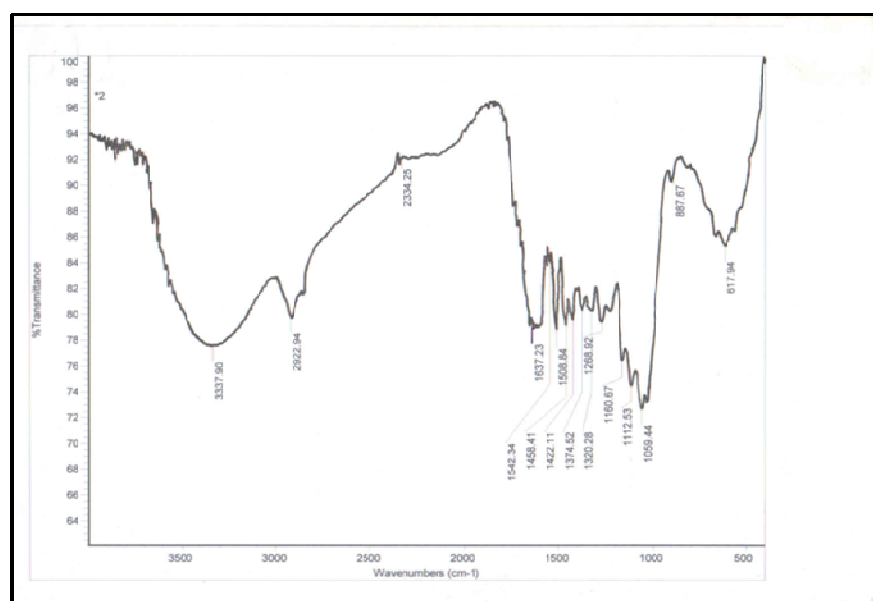


Figure 4.14 FT-IR spectrum of Ni (II) loaded TTCNS

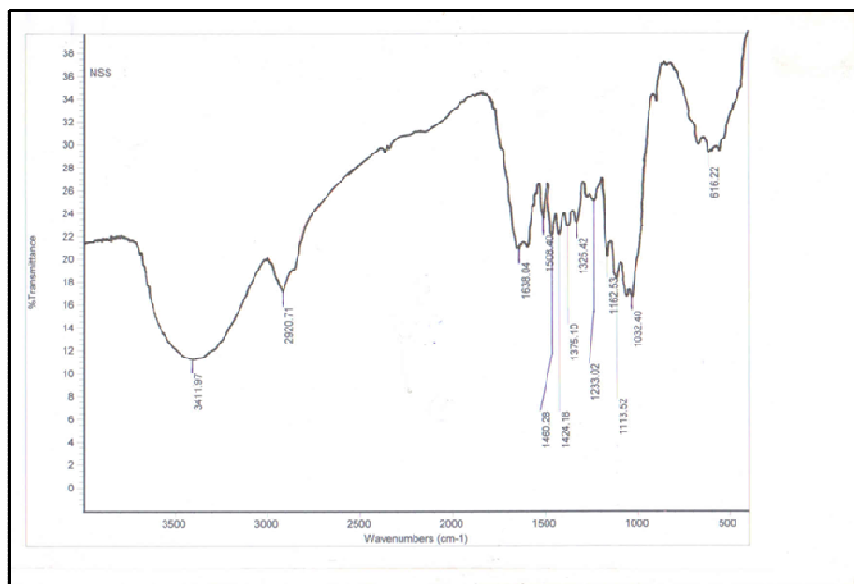


Figure 4.15 FT-IR spectrum of TAINS

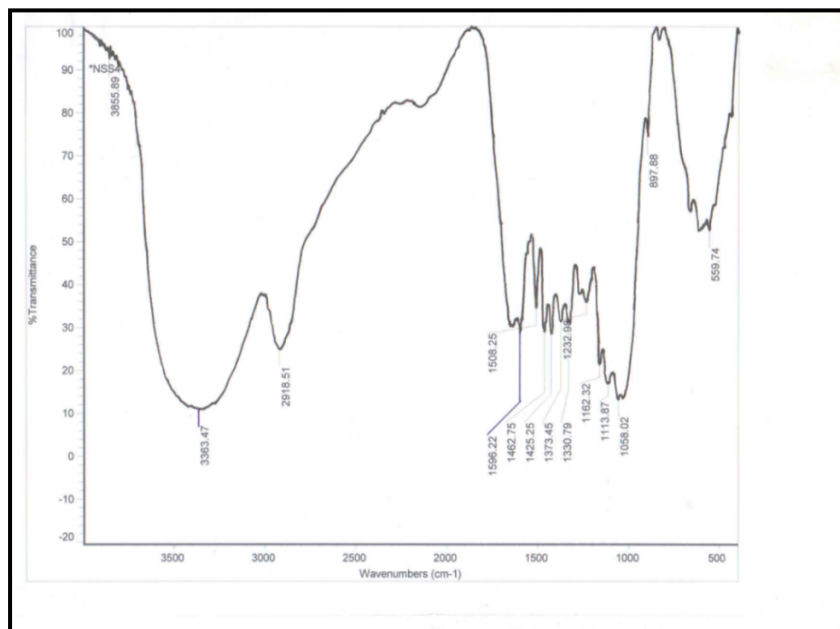


Figure 4.16 FT-IR spectrum of Ni(II) loaded TAINS